Forward-angle cross sections for pion-nucleon charge exchange between 100 and 150 MeV/c

D. H. Fitzgerald, H. W. Baer, J. D. Bowman, M. D. Cooper, F. Irom, N. S. P. King, M. J. Leitch, and E. Piasetzky*
Los Alamos National Laboratory, Los Alamos, New Mexico 87545

W. J. Briscoe
Department of Physics, George Washington University, Washington, D.C. 20052

M. E. Sadler and K. J. Smith
Department of Physics, Abilene Christian University, Abilene, Texas 79699

J. N. Knudson
Department of Physics, Arizona State University, Tempe, Arizona 85287
(Received 11 March 1986)

The differential cross sections for the πN charge-exchange reaction, $\pi^-p\rightarrow\pi^0n$, have been measured in an angular range corresponding to $0.99\geq\cos\theta_{c.m.}\geq 0.90$ at 100.6, 106.7, 113.4, 125.2, 130.9, 136.4, and 147.1 MeV/c. A striking feature of the charge-exchange reaction at forward angles is the presence of a deep minimum near 120 MeV/c, caused by interference between s- and p-wave scattering. The parameters of this minimum, of interest both intrinsically and for applications to π-nucleus single- and double-charge-exchange reactions, are well determined by the measurements. Our data are compared with the results of existing partial-wave analyses, and the data are discussed in terms of the isospin-odd, s-wave scattering length, a_1-a_3.

I. INTRODUCTION

The study of the pion-nucleon interaction at low energies has been of interest for many years. Experimentally obtained scattering amplitudes may be compared to specific predictions of a number of strong-interaction theories; this comparison has been carried out primarily in terms of the s-wave scattering lengths.[1-4] Measurement of the differential cross section for the πN charge-exchange reaction, $\pi^-p\rightarrow\pi^0n$, permits a determination of the isospin-odd, s-wave scattering length a_1-a_3. This quantity may also be indirectly deduced from πN measurements at higher energies by means of dispersion relations, by a measurement of the Panofsky ratio, or from mesic atom studies.[3]

It has been conjectured that charge-symmetry-breaking effects, which in the framework of quantum chromodynamics can arise from a difference of 4—6 MeV in the masses of the up and down quarks, could be appreciable in π^0N scattering near threshold.[4] However, the theoretical picture is much more complicated for $\pi^-p\rightarrow\pi^0n$ and the isospin-violating terms are expected to have a much smaller effect, although no quantitative calculations have been made. Indeed, early experimental results show apparent discrepancies between π^-p charge exchange and elastic scattering. More recently, it has been pointed out that the $u-d$ quark mass difference is small compared to the 500 MeV mass scale that determines the masses of the "dressed" quarks.[5] Consequently, this mass difference is expected to produce negligible isospin-violating effects in low-energy πN interactions.[6] Nevertheless, because isospin invariance is only "accidentally" obeyed, it is important to test this symmetry experimentally by measurements of πN elastic scattering and charge exchange at both low and high energies.

A specific feature of interest in the kinematic region of the present measurements is the prediction in partial wave analyses[7-9] of a deep minimum in the 0° differential cross section for $\pi^-p\rightarrow\pi^0n$ at a laboratory momentum in the range 120—130 MeV/c. The depth, width, and invariant mass of this minimum, which is due to nearly complete destructive interference between s- and p-wave scattering amplitudes, are sensitive to the parameters of the associated resonances in the pion-nucleon system. More recently, measurements of pion-nucleus single and double charge exchange at low energies have revealed features that place increased emphasis on determination of the pion-nucleon amplitudes.[10,11] In particular, very similar 0° minima have been observed at nearby momenta in the π-nucleus charge-exchange reaction to the isobaric analog state for a range of nuclear masses. This observation provides an opportunity for a detailed study of the effects of the nuclear medium on the πN interaction in a region not dominated by the Δ_{33} resonance; further, the distinctiveness of the sharp minimum in the πN cross section provides a "laboratory" for the study of two-particle properties in nuclei. πN data in this kinematic region are required as a basis for understanding this phenomenon.

Despite this interest, measurements of πN observables at low energies have been sparse, primarily because of ex-

perimental difficulties. The low-energy pion beams produced at meson factories are generally of low intensity and are highly contaminated by electrons and muons. For elastic scattering, losses of the final-state charged particles due to interactions in the target lead to large uncertainties in the cross section, especially for coincidence measurements. For charge exchange, the well-known problems associated with detection of the final-state photons and/or neutrons result in large systematic uncertainties in most cases. These difficulties include determination of the detection efficiency (particularly for neutrons) and rejection of background from both random sources and competing reactions such as radiative capture or photon production by stopped pions. To our knowledge, the only cross section measurements of the πN charge-exchange reaction at incident pion momenta below 150 MeV/c reported in the past 15 years are a measurement of the 180° cross section at 83, 101, and 117 MeV/c (Ref. 12) and a measurement of the integrated cross section at 90 and 112 MeV/c (Ref. 13).

In undertaking the present measurements we have been motivated both by the considerable scientific interest in the $\pi^-p\rightarrow\pi^0n$ reaction at low energy and the presence at the Clinton P. Anderson Meson Physics Facility (LAMPF) of a pion beam channel and detector eminently suited to this purpose. These are the low energy pion (LEP) channel and the LAMPF π^0 spectrometer. In particular, the π^0 spectrometer represents a considerable improvement over most other detectors in terms of solid angle, detection efficiency, and energy resolution. A crucial advantage of this detector is that reliable cross sections can be obtained by detecting only the π^0 in the final state. We report on measurements of the absolute differential cross section for the $\pi^-p\rightarrow\pi^0n$ reaction for $0.99\geq\cos\theta_{\text{c.m.}}\geq 0.90$ at pion beam momenta of 100.6, 106.7, 113.4, 125.2, 130.9, 136.4, and 147.1 MeV/c.

II. EXPERIMENT

The flux of negatively charged pions from the LEP channel ranged from 5×10^6 sec^{-1} at 100.6 MeV/c to 2×10^7 sec^{-1} at 147.1 MeV/c. The relative π^- beam intensity was monitored during each data run by means of a toroidal current monitor through which the primary proton beam passed. The absolute normalization of the pion intensity was established by measurements of the ^{11}C activity induced in scintillator disks placed at the target position, using the measured cross sections[14] for $^{12}C(\pi^{\pm},\pi N)^{11}C$. The uncertainty in the determination of the beam flux ranged from 4% to 8%, the contribution from the activation cross section dominating all others. The total π^- flux incident on the target at each beam momentum ranged from 1.4×10^{11} to 2.7×10^{11}. The transverse base-to-base dimensions of the beam at the target position, as observed in film exposures taken periodically, were typically 3.5 cm (horizontal) by 1.3 cm (vertical), well inside the area of the activation disks, which have a diameter of 5 cm. The rms divergence of the beam is estimated to have been 25 mrad vertically and 80 mrad horizontally, based on beam phase-space measurements for similar tunes of the LEP channel. The nominal central momentum of the channel has been determined to be correct to within an experimental uncertainty of 0.5% by measuring the energies of spallation particles with momentum 128 MeV/c from the pion production target.[15] The momentum acceptance setting of the channel, which was varied to produce an acceptable counting rate at each momentum, ranged from 1% (full width) at 147.1 MeV/c to 4% at 100.6 MeV/c.

The design, construction, and performance of the π^0 spectrometer are described in detail elsewhere.[16] However, we will describe briefly the features of the spectrometer that are important for the present discussion. Each of the photons from the decay of a π^0 is detected in one arm of the spectrometer. Each arm contains a "hardener" to absorb low-energy particles and photons, a thin scintillator counter to veto charged particle events, three converter planes, and a 3×5 array of total-absorption Pb-glass blocks. The hardener consists merely of a polyethylene sheet 3.6 g/cm^2 thick. The converter planes each consist of an active Pb-glass converter (area 64×40 cm^2, 0.58 radiation lengths thick), three multiwire proportional chamber (MWPC) planes, and a scintillation counter. The total-absorption blocks each have a face area of 15×15 cm^2 and a depth of 60 cm (14 radiation lengths). When a photon converts in one of the three planes, the conversion coordinates are determined from the MWPC information, the event timing is determined from the scintillators, and the energy is measured as the sum of the energy deposited in the converters and the blocks, which contain the full shower. The opening angle between the two photons is obtained from the MWPC information, assuming the vertex to be at the upstream center of the target; the π^0 energy and scattering angle in the laboratory frame is then obtained from the energies of the photons and the opening angle.

For all of the measurements presented here, the spectrometer remained in the same configuration. The detector arms were set symmetrically above and below the 0° direction with a vertical opening angle of 92.42°; the distance from the center of the target to the first conversion plane was 55 cm. This configuration optimized the acceptance of the spectrometer for a π^0 energy of 52 MeV (48.7 MeV or 126.3 MeV/c incident pions). The opening angle was measured in the vertical plane and the π^0 laboratory scattering angle in the horizontal plane; the uncertainty in the location of the photon conversion point was 6 mm FWHM (full width at half maximum) (vertical) by 1.2 mm FWHM (horizontal). Software cuts on the reconstructed conversion point defined the "fiducial area" (intrinsic solid angle) of each arm of the π^0 spectrometer to be 0.23 sr. The angular acceptance of the spectrometer for π^0's in this configuration was approximately 30° (laboratory). Software cuts were used to divide this acceptance interval into three scattering-angle bins: 0°–8°, 8°–16°, and 16°–30°.

Data for the $\pi^-p\rightarrow\pi^0n$ reaction were taken using a polyethylene (CH_2) target of areal density 1.165 g/cm^2. A typical π^0 energy spectrum, in this case for 136.4 MeV/c incident π^- momentum, is shown in Fig. 1 (solid circles). As can be seen, the π^0 peak from $\pi^-p\rightarrow\pi^0n$ is well resolved from the background (curve) produced by

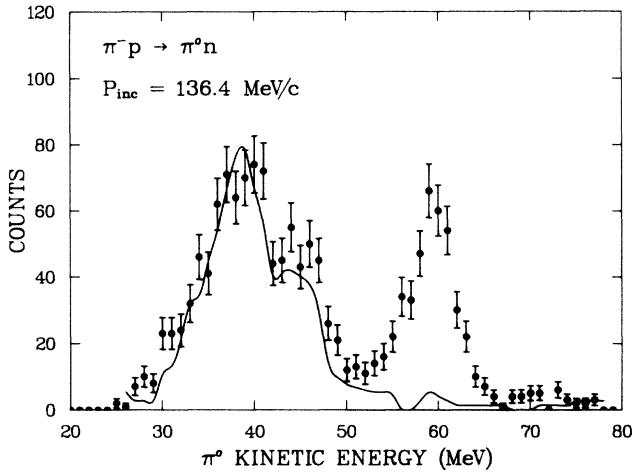

FIG. 1. π^0 energy spectrum for $\pi^- p \rightarrow \pi^0 n$ at an incident laboratory momentum of 136.4 MeV/c. The data points show the spectrum produced on a CH_2 (polyethylene) target and the solid curve shows the background spectrum obtained on a graphite target.

charge-exchange reactions on the carbon component of the target and on (primarily) air upstream and downstream of the target. The peak width is 5.5 MeV (FWHM); the contributions to this width come from the channel momentum bite (2.0 MeV), the π^- energy loss in the target (3.9 MeV), and the energy resolution of the π^0 spectrometer (3.0 MeV). The channel and target contributions to the momentum spread for each value of the π^- central momentum are listed in Table I. The background spectrum at each momentum was determined by separate runs on a graphite target whose areal density, 1.524 g/cm^2, was selected to give very nearly the same energy loss for the π^- beam as the CH_2 target. The background underlying the peak in Fig. 1 is 11% of the $\pi^- p \rightarrow \pi^0 n$ yield; the background-to-peak ratio ranges from 5% to 15%, except at 125.2 MeV/c, nearest the minimum, where it is 38% for the 0°—8° bin. The peak region includes the low-energy tail that remains following background subtraction; for example, the peak region in Fig. 1 is 52—77 MeV. The observed peak shape and width are consistent with those calculated in a Monte Carlo simulation.[16] The net yields in each bin (taken as counts in the peak after background subtraction) ranged from 150 to 1000 counts, the lowest yield being obtained near the minimum.

TABLE I. Contributions to the momentum width from the LEP channel momentum acceptance and the ionization momentum loss in the target (FWHM).

Central momentum (MeV/c)	Channel acceptance (MeV/c)	Target momentum width (MeV/c)
100.6	4.2	8.6
106.7	3.3	7.8
113.4	3.5	7.1
125.2	3.9	6.1
130.9	4.0	5.7
136.4	2.8	5.5
147.1	1.5	5.0

III. ANALYSIS

In addition to the MWPC software cuts that defined the fiducial area and the scattering-angle bins of the π^0 spectrometer, the data were subjected to cuts on the total energy of the two photons, the timing between the two arms, consistency of the tracks in the MWPC's, the direction of the most forward-going prong of the electromagnetic shower, and the energy-sharing parameter X. X is defined in terms of the photon energy measured in each of the two arms of the spectrometer: $X=(E_1-E_2)/(E_1+E_2)$. In the off-line analysis the effect of each of these cuts was thoroughly investigated to ensure that no valid events were excluded by any cut and that the cross sections remained consistent within the uncertainties implied by counting statistics when the cuts were varied. In particular, no unexpected variations were observed when the maximum value of $|X|$ was varied form 0.10 to 0.20; for the results presented here, $|X|$ values in the range 0—0.15 were accepted.

The solid angle, energy acceptance, and angular acceptance of the π^0 spectrometer were obtained in a Monte Carlo simulation[16] that takes into account the pion beam parameters (central momentum, momentum spread angular divergence, and transverse spot size), ionization energy loss and straggling in the target, finite-target-size effects, and the spectrometer parameters (X, the uncertainty in the photon conversion point, the spectrometer energy resolution, and the geometry). The π^0 solid angle obtained for each of the scattering-angle bins, respectively, was in the range 1.4—2.6 msr (0°—8°), 2.0—4.0 msr (8°—16°), and 0.6—1.7 msr (16°—30°) for the results presented here.

The photon detection efficiency of each converter plane was determined experimentally using the data acquired during the cross section measurements. For each plane this efficiency is, in principle, the product of the interaction probability for the photon in the Pb-glass converter and the probability that the interaction produces a detectable, forward-going charged particle. For the set of accepted events at each momentum, the events that passed all cuts in each of the three planes in each arm of the spectrometer were tabulated in a 3×3 matrix. Each of the matrix elements contained the number of events in which a given pair of converter planes satisfied all cuts, e.g., element (1,3) is the number of events in which the first plane in the first arm and the third plane in the second arm passed all cuts. The efficiency ϵ_c of a single plane was then obtained by a fit to all nine elements of the matrix by requiring that the relative efficiencies of the first, second, and third planes in each arm be given by ϵ_c, $(1-\epsilon_c)\epsilon_c$, and $(1-\epsilon_c)^2\epsilon_c$. The results of this procedure at all seven momenta are shown in Fig. 2 (solid circles). The error bars reflect only statistical uncertainties. The measurements are in good agreement with the results of a fit to Monte Carlo calculations[16,17] of ϵ_c (solid curve) and the results of calculations using a semiempirical formulation[18] of ϵ_c (dashed curve). The results of the two calculations mutually agree to within 1%. The agreement is not surprising because the relative thinness of the converters

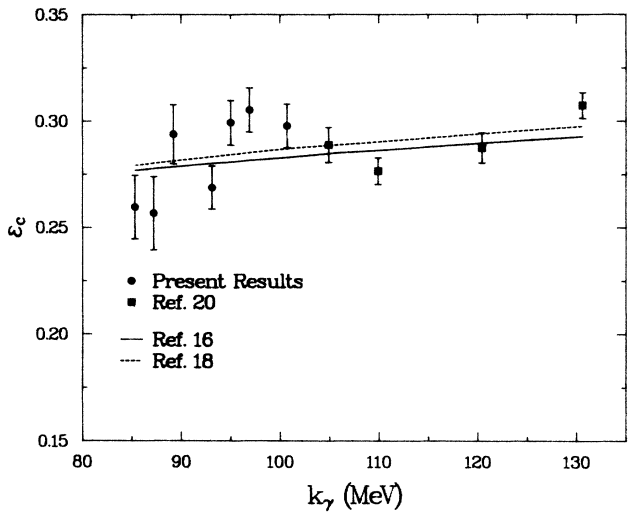

FIG. 2. Measurements and calculations of the single-plane conversion efficiency ϵ_c for the π^0 spectrometer (note offset origin). The solid circles are data obtained in the present experiment as described in the text, and the solid squares are data obtained in connection with the measurements of Ref. 20 by a comparison of $\pi^-p\to\pi^0n$ yields to cross sections from partial wave analyses. The solid curve is a fit to a Monte Carlo calculation described in Ref. 16 and the dashed curve is the result of a semiempirical calculation (Ref. 18).

reduces the electron reabsorption probability to 1—2%; therefore, the detection efficiency (probability of producing a detectable charged particle) is very nearly equal to the photon interaction probability, which is known to 1%.[19] Reasonable agreement between the measurements and the calculations is seen in Fig. 2; the rms variance of the data from the solid curve is 0.0156 (5.6%). For the cross sections presented here, the fit to the Monte Carlo calculation is used to determine ϵ_c and a normalization uncertainty of 5.6% is adopted. Finally, Fig. 2 also contains four experimental points (solid squares) that were obtained at higher photon energies in measurements[20] taken shortly after the present experiment. The results in this case were obtained by taking the ratio of measured yields for $\pi^-p\to\pi^0n$ to cross sections determined in a partial wave analysis,[8] and are only shown here to illustrate their consistency with the energy dependence observed for both the present measurements and the calculations. The overall π^0 detection efficiency, $\epsilon(\pi^0)$, is given by

$$\epsilon(\pi^0)=[1-(1-\epsilon_c)^3]^2 . \quad (1)$$

The 5.6% uncertainty in the determination of ϵ_c leads to a 7.8% normalization uncertainty in $\epsilon(\pi^0)$.

Note that the experimental determination of ϵ_c, the efficiency for a single converter plane, depends only on the ratios of the numbers of accepted events among all six converted planes. The determination of ϵ_c does not depend on the charged-particle detection efficiencies of the scintillators, Pb-glass converters, and MWPC's, to the degree that these do not differ significantly from plane to plane. This condition is satisfied, since the charged-particle detection efficiency was separately measured to be $\geq 99\%$ for each scintillator, Pb-glass converter, and MWPC in the π^0 spectrometer. The track-reconstruction efficiency is also excluded from the experimental determination of ϵ_c because only those events having acceptable tracks were used in the calculation. The product of the charged-particle detection efficiencies and the track-reconstruction efficiency was determined during the course of each data run. This efficiency product, ϵ_W, ranged from 0.78 to 0.85.

IV. CROSS SECTION CALCULATION

Differential cross sections for $\pi^-p\to\pi^0n$ in the c.m. system were calculated from the measurements using the expression

$$\frac{d\sigma}{d\Omega}(\text{c.m.})=\frac{YJ}{N(\pi^-)N_H\Omega(\pi^0)\epsilon(\pi^0)\epsilon_W f_{\text{abs}}F_{\gamma\gamma}\tau_L} , \quad (2)$$

where Y is the net number of events in the peak following background subtraction, J is the Jacobian of the transformation of the differential cross section from the laboratory to the c.m. system, $N(\pi^-)$ is the number of π^-'s incident on the target, N_H is the number of hydrogen atoms per cm^2 in the target, $\Omega(\pi^0)$ is the laboratory solid angle of the spectrometer for π^0's, $\epsilon(\pi^0)$ is the π^0 detection efficiency, ϵ_W is the product of the scintillator, Pb-glass and MWPC detection efficiencies, and the track reconstruction efficiency, f_{abs} is the fraction of the photons not absorbed in the target, the polyethylene "hardener," and the veto detector (typically 0.856), $F_{\gamma\gamma}$ is the $\pi^0\to\gamma\gamma$ branching ratio (0.988 02), and τ_L is the experimental livetime (range 0.77—0.89).

The momentum interval associated with each data point is the quadrature sum of the channel momentum acceptance and the ionization momentum loss in the target. This momentum interval ranged from 5.2 MeV/c at 147.1 MeV/c to 9.6 MeV/c at 100.6 MeV/c (see Table I). In order to obtain the true differential cross section at each momentum for each of the three angle bins, the measured results were corrected for the variation of the cross section within the momentum interval. The correction procedure involved expansion of the cross section in a Taylor's series as a function of laboratory momentum. The terms in the Taylor's series were then estimated from a power series fit to the measured data. Because the fit to the data was not improved by the addition of terms higher than fourth order, both the power series and the Taylor series were truncated at five terms. The process was iterated using the corrected data until convergence, defined as less than 0.1% change in any of the cross sections in a single step, was reached. Convergence occurred on the second step in all cases. The largest correction, 5.6%, was obtained for the most forward angle bin at 125.2 MeV/c. Far from the minimum the corrections were $\leq 1\%$. The systematic uncertainty in each cross section resulting from the correction is estimated to be less than 1%, except for the points at the minimum, where 1.5—2% is appropriate. In any case, this uncertainty makes a negligible contribution when added in quadrature to the statistical uncertainty and the other systematic uncertainties.

The final results were extrapolated to 0° using a second-order polynomial in $\cos\theta_{\text{c.m.}}$ (comparison to a

TABLE II. Differential cross sections in the c.m. vs laboratory momentum for the pion-nucleon charge-exchange reaction. The first uncertainty listed in each case contains the uncertainties in counting statistics and detector solid angle; the second includes the additional momentum-dependent systematic uncertainties discussed in the text. There is also an overall normalization uncertainty of 7.8%.

Momentum (MeV/c)	$\cos\theta$	$d\sigma/d\Omega$ (μb/sr)
100.6	1.000	42.2±3.8 (5.1)
	0.985	44.1±3.3 (4.6)
	0.968	47.9±2.9 (4.5)
	0.920	54.3±4.4 (5.9)
106.7	1.000	22.4±2.6 (3.0)
	0.984	26.1±2.3 (2.8)
	0.965	32.9±2.1 (3.0)
	0.917	44.5±3.9 (4.8)
113.4	1.000	8.6±1.1 (1.2)
	0.985	12.5±1.1 (1.3)
	0.963	17.9±1.0 (1.5)
	0.917	29.8±1.9 (2.6)
125.2	1.000	4.48±.78 (.86)
	0.985	7.48±.78 (.99)
	0.962	10.6±0.7 (1.1)
	0.916	19.8±1.3 (2.1)
130.9	1.000	12.0±1.1 (1.3)
	0.986	15.7±1.1 (1.5)
	0.962	15.2±0.9 (1.4)
	0.913	25.7±1.6 (2.3)
136.4	1.000	25.8±1.7 (2.3)
	0.986	27.4±1.7 (2.4)
	0.961	30.5±1.6 (2.4)
	0.908	36.7±2.4 (3.3)
147.1	1.000	73.3±4.0 (5.5)
	0.986	75.6±3.9 (5.5)
	0.961	71.6±4.2 (6.0)
	0.906	77.4±3.2 (5.1)

first-order fit gave a difference in the 0° result of less than 0.3% in the worst case). As a consistency check, 0° cross sections were also obtained by reversing the order of correction and extrapolation; that is, first extrapolating the raw data to 0° and then applying the correction for momentum interval. This check resulted in excellent agreement; the largest difference in any 0° cross section between the two methods is 1%.

V. RESULTS AND DISCUSSION

The differential cross sections in the c.m. system for the reaction, $\pi^-p\to\pi^0n$, for each of the three angle bins plus the extrapolated value at $\cos\theta=1.0$ are listed for each π^- laboratory momentum in Table II. The first uncertainty shown contains the contributions from counting statistics and $\Omega(\pi^0)$; the second value, in parentheses, includes, in addition, the contributions from $N(\pi^-)$, ϵ_W, and τ_L at each momentum. The uncertainties for the cross sections at $\cos\theta=1.0$ also include the contribution from the extrapolation uncertainty. Finally, there is an overall normalization uncertainty of 7.8% in the determination of $\epsilon(\pi^0)$ that applies to all the cross sections.

The differential cross sections for each of the three angle bins ($\cos\theta=0.99$, 0.96, and 0.91) are plotted in Fig. 3 versus c.m. momentum. The error bars reflect the second uncertainties listed in Table II, as described in the preceding paragraph. There is, of course, also a scale-factor uncertainty of 7.8%. The data at all three angles exhibit a minimum near 100 MeV/c, caused by the nearly complete cancellation of the s- and p-wave amplitudes that dominate the πN interaction at this momentum. The depth of the minimum decreases rapidly with increasing angle (decreasing $\cos\theta$). This behavior can be understood by considering the spin-non-flip amplitude $g(\theta,p)$ and the spin-flip amplitude $h(\theta,p)$ at the momentum $p_{\min}$ of the cross section minimum. Because only the s and p waves contribute, g and h are given by

$$g(\theta,p)=g_0(p)+g_1(p)\cos\theta\,, \tag{3}$$

$$h(\theta,p)=h_1(p)\sin\theta\,. \tag{4}$$

At $\cos\theta=0.99$ the spin-flip amplitude vanishes and $g_0(p_{\min})$ must nearly cancel $g_1(p_{\min})$. Typical values[3,8,21] for the real parts of g_0, g_1, and h_1 at $p_{\min}$ are -0.175, 0.17, and 0.10 fm, respectively. The imaginary parts of the amplitudes are less than 10% of the real parts and so contribute negligibly to the cross section. The decrease of $\cos\theta$ from 0.99 to 0.91 thus gives rise to an increase in $g(\theta,p_{\min})$ of only a factor of 2, producing a 50% increase in the cross section. Clearly, the filling in of the

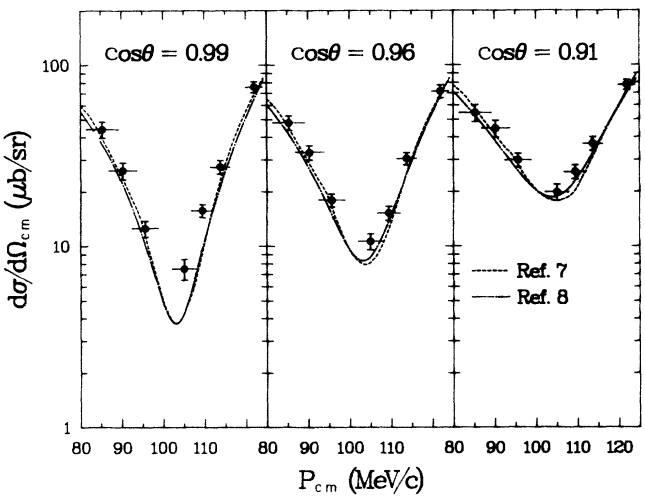

FIG. 3. Differential cross sections for $\pi^-p\to\pi^0n$ at $\cos\theta=0.99$, 0.96, and 0.91 vs momentum in the c.m. system. The error bars reflect the quadrature sum of the uncertainties in counting statistics, detector solid angle, and the beam flux measurement at each momentum. An overall normalization uncertainty of 7.8%, not included in the error bars, also applies to these data. The dashed curves are the results of a PWA analysis by the KH group (Ref. 7) and the dotted-dashed curves are those of the VPI group (Ref. 8).

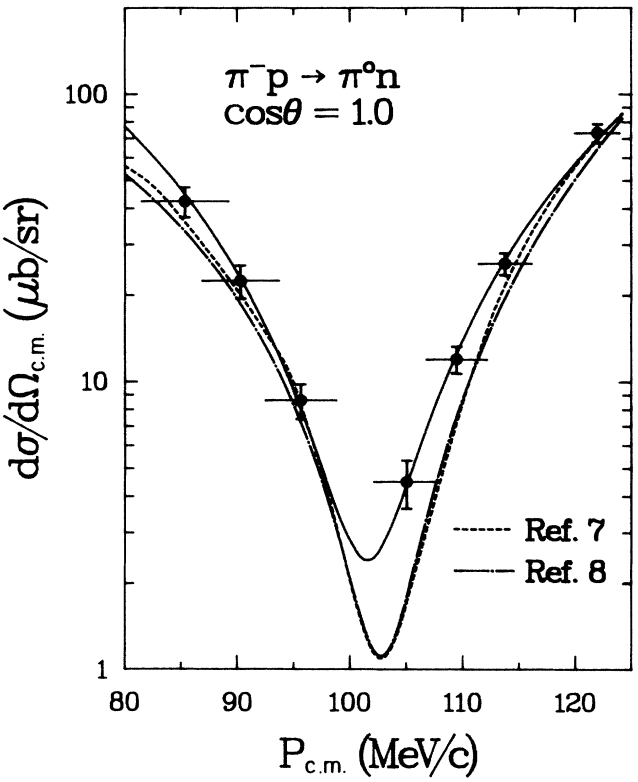

FIG. 4. Differential cross sections for $\pi^- p \rightarrow \pi^0 n$ at $\cos\theta = 1.0$, obtained by extrapolating the measured cross sections in Table II. The error bars reflect the quadrature sum of the three uncertainties used in Fig. 3 and the extrapolation uncertainty. As in Fig. 3, a 7.8% overall normalization uncertainty also applies to these data. The solid curve is the result of a fit to the plotted cross sections of the form $d\sigma/d\Omega = 1664.3 - 32.740p + 0.161\,25p^2$, where p is the π^- c.m. momentum. The dashed curve is the result of a PWA by the KH group (Ref. 7) and the dotted-dashed curve is that of the VPI group (Ref. 8).

minimum comes from the spin-flip term, whose contribution to the cross section increases by a factor of 8.6 between $\cos\theta = 0.99$ and 0.91.

Our extrapolated results at $\cos\theta = 1.0$ are plotted in Fig. 4 together with a fit of the form $d\sigma/d\Omega = a + bp + cp^2$ (solid curve), where p is the c.m. momentum. The values obtained for the coefficients in the fit are $a = 1664.3$, $b = -32.740$, and $c = 0.16125$. This fit has a χ^2 of 0.6 per degree of freedom; the minimum in the fitted curve occurs at 101.5 ± 0.6 MeV/c and has a magnitude of 2.4 ± 0.5 μb/sr. The uncertainty in the momentum at which the minimum occurs takes into account the contributions from counting statistics, the fitting procedure, and the uncertainty in the central momentum of the LEP channel. The uncertainty in the value of the cross section at the minimum includes the contributions from these three sources and the systematic uncertainties in $N(\pi^-)$, $\Omega(\pi^0)$, ϵ_W, τ_L, and $\epsilon(\pi^0)$.

Also shown in Figs. 3 and 4 are the results of two recent partial wave analyses (PWA's) by the groups from Karlsruhe-Helsinki[7] (KH, dashed curve) and Virginia Polytechnic Institute[8] (VPI, dotted-dashed curve). Neither of these analyses includes the present results. As can be seen in Fig. 3, the PWA results are in good mutual agreement and represent the data at $\cos\theta = 0.91$ reasonably well. However, as the depth of the minimum increases at $\cos\theta = 0.96$ and 0.99, the agreement of the PWA results with the data becomes poorer in the region of the minimum and, to a lesser degree, at momenta above the minimum. At $\cos\theta = 1.0$ the minimum is at its deepest and the disagreement between the PWA results and the (extrapolated) data is at a maximum, as can be seen in Fig. 4. The parameters of the minimum obtained in the two analyses are 1.08 μb/sr at 102.8 MeV/c (KH) and 1.14 μb/sr at 102.4 MeV/c (VPI). The PWA values for the cross section at the minimum thus disagree with the measured result by a factor of 2.2 and the predicted location of the minimum is too high by approximately 1 MeV/c. The disagreement between the PWA results and our data may contain implications for the low-energy scattering amplitudes obtained in the partial wave analyses. However, the quantitative importance of the disagreement can be assessed only by a new PWA which includes our data.

As mentioned in the Introduction, measurement of the differential cross section for the πN charge-exchange reaction permits, in principle, a determination of the isospin-odd, s-wave scattering length $a_1 - a_3$. However, a difficulty in using the present data alone to obtain $a_1 - a_3$ is that the p-wave amplitude is comparable to that of the s-wave at these momenta. Thus, one must measure a complete angular distribution at a given momentum or, for the present data, which have a very limited angular range, fit the data with a function of momentum and angle in order to determine the pure s-wave contribution. Siegel and Gibbs[21] have recently completed an analysis of low-energy charge-exchange and elastic scattering πN data, using nonlocal potentials in a coupled-channels approach. They have varied the range and strength of the isospin $\frac{1}{2}$ potentials to the existing charge-exchange data including our results. These authors point out that the relative s- and p-wave amplitudes can be very accurately obtained from the charge-exchange data at the point of near cancellation ($p = p_{\min} = 101.5$ MeV/c, $\theta = 0°$). This can be seen from the low-energy forms used by Siegel and Gibbs for the real parts of $g(\theta,p)$ and $h(\theta,p)$:

$$g(\theta,p) = a + bp^2 + cp^2\cos\theta, \tag{5}$$

$$h(\theta,p) = dp^2\sin\theta, \tag{6}$$

where $a = a_1 - a_3$. (The bp^2 term in the expression for g is needed to account for the large effective range of the $s_{1/2}$ amplitude.) As noted above, the spin-flip amplitude is zero at 0° for all values of p and $g(0,p_{\min}) \rightarrow 0$, so $a + (b+c)p_{\min}^2 \rightarrow 0$. In a fit to our 21 data points plus the five data points of Refs. 12 and 13, Siegel and Gibbs obtain for $a = a_1 - a_3$ the minimum χ^2 value: $0.290 \pm 0.005\mu^{-1}$. Although this determination of the isospin-odd, s-wave scattering length is based directly on measurements of the $\pi^- p \rightarrow \pi^0 n$ cross section at low momenta, it clearly contains model assumptions that introduce uncertainties whose magnitudes are difficult to assess.

In Table III we compare the value of $a_1 - a_3$ obtained by Siegel and Gibbs, based primarily on the present results, to values obtained using a variety of methods. Any

TABLE III. Experimental determinations of a_1-a_3.

Method	a_1-a_3 (μ^{-1})	Ref.
Potential model fit to present results plus five points from Refs. 12 and 13	0.290±0.005	21
$\pi^-p\to\pi^0n$ 180° cross sections	0.291±0.024 (83 MeV/c) 0.284±0.023 (101 MeV/c) 0.242±0.023 (117 MeV/c)	2
Fit to single-photon data for $\pi^-p\to\pi^0n$	0.260±0.012 (92 MeV/c) 0.265±0.012 (112 MeV/c)	13
Extrapolate partial waves, fit to effective-range expansion	0.240 0.283±0.008	8 9
Dispersion-relation evaluation of scattering amplitudes	0.274±0.005 0.262±0.004 0.275±0.004	7 23 24
Panofsky ratio	0.263±0.005	22
Pionic atoms	0.258±0.008	28

discussion of the differences among the values of a_1-a_3 in Table III clearly must include a consideration not only of the experimental data, but also of the assumptions employed in proceeding from the measurements to the scattering length value. Only the values obtained by Duclos *et al.*[12] are based on direct measurements of the $\pi^-p\to\pi^0n$ cross sections at low momenta; however, because these authors measured only the 180° cross section, they were forced to rely on existing PWA results to extract the p-wave contribution to the scattering. Given the quality of then-existing πN data, it is not clear that this technique leads to a reliable value for a_1-a_3; in any case, the values obtained by Duclos *et al.* contain a momentum dependence that is considerably outside the quoted uncertainties. The values obtained by extrapolation of the scattering amplitudes from higher energies (Refs. 7, 23, and 24) make substantial use of analytic constraints in the form of dispersion relations, and rely primarily on data for $\pi^\pm p$ elastic scattering from a wide variety of sources, leaving open the question of relative normalization and systematic errors. Similar questions concerning the method of extrapolation and the database question also pertain to the values obtained by extrapolations of partial waves from higher energies (Refs. 8 and 9). In addition, the range of validity of the effective range expansion has been called into question[3] in regard to these values. Siegel and Gibbs have discussed in some detail the results obtained in Ref. 13 and those obtained by means of a measurement of the Panofsky ratio (Ref. 22); they ascribe differences between their results and those of Ref. 13 to the method used to extrapolate the charge-exchange cross section from finite energy to zero energy. The determination of the Panofsky ratio between the threshold cross sections for $\pi^-p\to\pi^0n$ and $\pi^-p\to\gamma n$ is very precise:[22] However, the determination of a_1-a_3 from the Panofsky ratio also depends on the threshold ratio R between the cross sections for $\gamma n\to\pi^-p$ and $\gamma p\to\pi^+n$,[25] and on the value[26] of the s-wave multipole, $E_{0+}(\pi^+)$. R is obtained from photoproduction measurements on deuterium by applying corrections for Coulomb effects and the effects of the spectator nucleon; it is difficult to judge whether the uncertainties in these corrections are estimated accurately. Further, E_{0+} is obtained by extrapolation to threshold of cross sections for $\gamma p\to\pi^+n$ measured[27] at 165–230 MeV with uncertainties ranging from 7% to 20%. The uncertainties contained in this extrapolation can easily account for differences between the "Panofsky ratio" value for a_1-a_3 and those obtained from πN cross sections, as Siegel and Gibbs show.[21] Finally, there is the value of a_1-a_3 obtained from measurements of the width and shift in the $1s$ level in pionic atoms.[28] While these measurements can apparently be made to very high precision, the determination of a_1-a_3 is based on parameter fitting in an optical potential model for atomic masses greater than ten.

We would only add the following two points concerning Table III: First, the value obtained by Siegel and Gibbs lies just within the rather broad range of values resulting from previous determinations of a_1-a_3 (0.24–0.29); second; the quoted uncertainties in the values (typically ±0.004 to ±0.007) are remarkably small considering the large scatter in the values, which have a rms variance of approximately 0.02. Given the fundamental nature of the isospin-odd, s-wave scattering length and its importance as a value predicted by low-energy models of the πN system on the basis of PCAC (partially conserved axial-vector current) in the soft-pion limit,[2] this confusion in the experimentally determined values is unfortunate. A precise measurement of the cross sections for $\pi^-p\to\pi^0n$ over a wide range of scattering angles at momenta close to the threshold would avoid many of the limitations discussed above and would constitute a very nearly direct experimental determination of a_1-a_3. Such a measurement has been undertaken at LAMPF by a group including many of the present authors and preliminary results are expected within the next six months.

The investigation of isospin invariance by a comparison of isospin $\frac{1}{2}$ and $\frac{3}{2}$ amplitudes obtained from π^+p and π^-p elastic scattering and from π^-p charge exchange is hampered by a lack of consistency among the elastic scattering results. The analysis of Siegel and Gibbs suggests that the assumption of isospin invariance is not in-

consistent with the bulk of the existing data. A quantitative investigation of isospin invariance must await improved elastic scattering data (and, perhaps, more extensive charge exchange measurements) at low momenta.

In summary, we have measured the cross section for the reaction $\pi^-p \rightarrow \pi^0 n$ at small scattering angles in the momentum range which contains a steep minimum caused by near cancellation of the s- and p-wave amplitudes. The 0° cross section extrapolated from our results gives a minimum whose magnitude is a factor of 2 larger than the predictions of existing partial wave analyses; the location of the minimum obtained from the present results is 1 MeV/c lower than the PWA predictions. An analysis based largely on our results obtains a value for the isospin-odd, s-wave scattering length which is consistent with the range of values obtained in other, less direct determinations. The precision of the present results and of elastic scattering data and the inconsistencies among the elastic scattering results preclude a meaningful investigation of isospin invariance.

ACKNOWLEDGMENTS

We thank the technical staff at LAMPF for their able support of this experiment. We are grateful to R. A. Arndt and L. D. Roper and to R. Koch and G. Höhler for making available their respective interactive phase shift codes. Finally, we thank W. R. Gibbs and P. B. Siegel for several helpful discussions of their analysis of low-energy πN elastic scattering and charge exchange. This work was supported in part by the United States Department of Energy and the National Science Foundation.

*Present address: Physics Department, Tel Aviv University, Tel Aviv, Israel.

[1]S. Weinberg, Phys. Rev. Lett. **17**, 616 (1966).

[2]S. Fubini and G. Furlan, Ann. Phys. (N.Y.) **48**, 322 (1968).

[3]G. Höhler, in *πN Scattering: Phenomenological Analysis,* Vol. 9b2 of *Landolt-Börnstein New Series,* edited by H. Schopper (Springer-Verlag, Berlin, 1983), and references therein.

[4]S. Weinberg, Trans. N.Y. Acad. Sci. **38**, 185 (1977).

[5]Nathan Isgur, Phys. Rev. D **21**, 779 (1980).

[6]R. E. Cutkosky, Phys. Lett. **88B**, 339 (1979).

[7]R. Koch and E. Pietarinen, Nucl. Phys. **A336**, 331 (1980); G. Höhler and R. Koch, interactive phase shift program.

[8]R. A. Arndt, J. M. Ford, and L. D. Roper, Phys. Rev. D **32**, 1085 (1985); R. A. Arndt and L. D. Roper, phase shift program SAID.

[9]G. Rowe, M. Salomon, and R. H. Landau, Phys. Rev. C **18**, 584 (1978).

[10]F. Irom, M. J. Leitch, H. W. Baer, J. D. Bowman, M. D. Cooper, B. J. Dropesky, E. Piasetsky, and J. N. Knudson, Phys. Rev. Lett. **55**, 1862 (1985).

[11]W. R. Gibbs, W. B. Kaufmann, and P. B. Siegel, in Proceedings of the LAMPF Workshop on Pion Double Charge Exchange, Report No. LA-10550, edited by H. W. Baer and M. J. Leitch, 1985.

[12]J. Duclos, A. Gerard, A. Magnon, J. Miller, J. Morgenstern, P. Y. Bertin, B. Coupat, J. C. Montret, B. Michal, and P. Vernin, Phys. Lett. **43B**, 245 (1973).

[13]M. Salomon, D. F. Measday, J.-M. Poutissou, and B. C. Robertson, Nucl. Phys. **A414**, 493 (1984).

[14]G. W. Butler, B. J. Dropesky, C. J. Orth, R. E. L. Green, R. G. Korteling, and G. K. Y. Lam, Phys. Rev. C **26**, 1737 (1982).

[15]M. V. Hoehn and D. H. Fitzgerald, LAMPF Report No. A82-01, 1982 (unpublished).

[16]H. W. Baer, R. D. Bolton, J. D. Bowman, M. D. Cooper, F. H. Cverna, R. H. Heffner, C. M. Hoffman, N. S. P. King, J. Piffaretti, J. Alster, A. Doron, S. Gilad, M. A. Moinester, P. R. Bevington, and E. Winkelman, Nucl. Instrum. Methods **180**, 445 (1981).

[17]S. Gilad, Ph.D. thesis, Tel Aviv University, 1979 (unpublished).

[18]D. I. Sober, Nucl. Instrum. Methods **166**, 555 (1979), and private communication.

[19]J. H. Hubbell, Photon Cross Sections, Attenuation Coefficients, and Energy Absorption Coefficients from 10 keV to 100 GeV, NSRDS-NBS **29** (1969).

[20]F. Irom, J. D. Bowman, H. W. Baer, E. Piasetzky, and J. Alster (unpublished).

[21]P. B. Siegel and W. R. Gibbs, Phys. Rev. C **33**, 1407 (1986).

[22]J. Spuller, D. Berghofer, M. D. Hasinoff, R. MacDonald, D. F. Measday, M. Salomon, T. Suzuki, J.-M. Poutissou, R. Poutissou, and J. K. P. Lee, Phys. Lett. **67B**, 479 (1977).

[23]D. V. Bugg, A. A. Carter, and J. R. Carter, Phys. Lett. **44B**, 278 (1973).

[24]R. Koch, Nucl. Phys. **A448**, 707 (1986).

[25]M. I. Adamovitch, V. G. Larionova, and S. P. Kharlamov, Yad. Fiz. **20**, 55 (1974) [Sov. J. Nucl. Phys. **20**, 28 (1975)].

[26]M. M. Nagels, Th. A. Rijken, J. J. deSwart, G. C. Oades, J. L. Peterson, A. C. Irving, C. Jarlskog, W. Pfeil, H. Pilkuhn, and H. P. Jakob, Nucl. Phys. **B147**, 189 (1979).

[27]M. I. Adamovitch, V. G. Larionova, S. P. Kharlamov, and F. R. Yagudina, Yad. Fiz. **7**, 579 (1968) [Sov. J. Nucl. Phys. **7**, 360 (1968)]; M. I. Adamovitch, V. G. Larionova, S. P. Kharlamov, and F. R. Yagudina, *ibid.* **9**, 848 (1969) [**9**, 496 (1969)].

[28]L. Tauscher and W. Schneider, Z. Phys. **271**, 409 (1974).